International Journal of Astrobiology 7 (2): 157–167 (2008) Printed in the United Kingdom
doi:10.1017/S1473550408004205 © 2008 Cambridge University Press

On the forcing mechanism for the H_2-driven deep biosphere

Helge Hellevang

Center for Geobiology at Department of Earth Sciences, University of Bergen, Allègaten 41, 5007 Bergen, Norway
e-mail: helge.hellevang@geo.uib.no

Abstract: Heat produced in the mantle and core of the Earth by the decay of radioactive elements and mineral fusion results in large-scale mantle convection. The outer shell of the Earth that floats on the convective mantle is divided into rigid lithospheric plates. Subduction of dense cold plates into the mantle leads to plate tectonics. At divergent plate margins, heat is dissipated through hydrothermal convection cells. As ocean water is entrained into hydrothermal cells it interacts with fresh magmatic rocks and liberates ferrous iron. This iron reduces the ocean water to such an extent that it decomposes and forms hydrogen. Molecular hydrogen, as the most reduced component in the system, forms a basal component to a deep dark biosphere powered by metastable redox gradients. In this paper we review the driving force behind a hydrogen-driven deep biosphere. We present abundant observations of hydrogen produced at natural hydrothermal settings as well as in laboratory experiments. The key mineral reactions responsible for the bulk of this hydrogen production are then presented. A division of the reaction progression into an oxidized state and a reduced state is suggested. The amount of hydrogen produced is insignificant in the oxidized state whereas it becomes proportional to the amount of ferrous iron oxidized in the reduced state. The bulk of basalt-hosted aquifers are expected to reside in the oxidized state because of the low content of ferrous minerals, whereas abundant olivine in ultramafic-hosted systems is responsible for large-scale hydrogen production. Today the majority of the seafloor is basaltic. The Archean seafloor on the other hand consisted of fewer ultramafic exposures, but was dominated by ultramafic magnesium-rich lavas with a higher potential for hydrogen production than the present seafloor.

Received 4 April 2008, accepted 2 May 2008, first published online 8 July 2008

Key words: Hydrogen, deep biosphere, serpentinization, Olivine, hydrothermal, black smoker.

Introduction

Prior to the late 1980s scientists considered it unlikely that communities of microbes could colonize what were considered nutrient-poor 'harsh' deep environments, even though microbes had earlier been observed in deep marine sediments and groundwater samples (Fliermans & Balkwill 1989). A program established by the US Department of Energy (DOE) in 1985 sought to extend the knowledge of subsurface microorganisms. Abundant diverse microbial communities were sampled from boreholes down to 520 m beneath the soil surface (e.g. Fliermans 1989; Fliermans & Balkwill 1989; Jiménez 1990). An extensive array of independent reports has since then extended our knowledge of the widespread subsurface deep biosphere. Microbes from a large variety of environments, at extreme temperatures, salinities, pressures, and acidities, have been added to the tree of life (e.g. Schleper *et al.* 1995; Ventosa *et al.* 1999; Kashefi & Lovley 2003; Marion *et al.* 2003; Junge *et al.* 2004; Torsvik & Øvreås 2008). Living prokaryotic cells have recently been reported (Roussel *et al.* 2008) discovered at depths down to 1626 mbsf (metres below the seafloor). Moreover, gene sequences and microbial isolates from a wide variety of different subsurface lithologies have been characterized, including: the seafloor (e.g. Cowen *et al.* 2003; Kimura *et al.* 2003; Lysnes *et al.* 2004; Schippers *et al.* 2005), marine sediments (e.g. Parkes *et al.* 1994; Hinrichs *et al.* 1999; Kormas *et al.* 2003; Toffin *et al.* 2004; Schippers & Neretin 2006), and terrestrial rocks (e.g. Kotelnikova & Pedersen 1997; Pedersen 2001).

Microbes in the deep biosphere encompass a wide range of energy metabolisms such as sulphate reduction, methanogenesis, methane oxidation, and aerobic respiration (e.g. Teske *et al.* 2003; Schippers *et al.* 2005; Schippers & Neretin 2006; Wortmann *et al.* 2007). Hydrogen, as a strongly reduced component, is an integral part of many of these metabolic pathways and is a basal component of the deep biosphere. The basal nature of hydrogen in these systems suggests that the deep biosphere is to some extent dependant on hydrogen. In this context, the hydrogen-driven deep biosphere is defined as a subsurface syntrophic biosphere with hydrogen as its basal component. Nealson *et al.* (2005) distinguished between hydrogen-facilitated and hydrogen-driven ecosystems. The former involves metabolism where hydrogen is produced by one organism and a syntrophic

https://doi.org/10.1017/S1473550408004205 Published online by Cambridge University Press

partner that removes hydrogen is needed to facilitate the overall ecosystem, whereas the latter is driven by oxidation of hydrogen by oxygen or other photosynthetically produced oxidants or geologically supplied oxidants such as carbon dioxide (Nealson *et al*. 2005). Subsurface lithoautotrophic microbial ecosystems (SliMEs) are geologically powered dark ecosystems that operate without any influence from photosynthesis (Nealson *et al*. 2005). The term hydrogen-driven deep biosphere as used in this review is broad and covers both hydrogen-facilitated and hydrogen-driven ecosystems as defined by Nealson *et al*. (2005).

About two-thirds of the Earth's outer rigid shell is made of an oceanic lithosphere (Karson 2001) consisting of reduced mafic and ultramafic rocks. Fresh unweathered material is constantly supplied at divergent plate boundaries and at so-called mantle hot spots. The fresh reduced material is highly reactive in contact with seawater at the ocean-floor pressures and temperatures. It is at the interface between the hydrosphere and the reduced magmatic rocks that hydrogen forms. The driving mechanism for the deep biosphere is the dissipation of energy from the inner Earth. Moreover, without the plate tectonics that drives element cycling the Earth would eventually be a lifeless planet.

This paper provides a review of the driving force behind plate tectonics, hydrothermal convection, and life on Earth. As hydrothermal vents can be regarded as point sources of elevated hydrogen production some representative hydrothermal vent sites together with hydrothermal laboratory experiments provide evidence for the hydrogen production. A theoretical section then gives insight into the reactions that are responsible for hydrogen formation in these environments, and the limiting factors for these reactions and reaction rates. As organic molecules are fundamental parts of the present-day deep biosphere and necessary constituents for the Archean emergence of life, the role of hydrogen in the synthesis of some organic molecules is also discussed. The last part covers the present-day global hydrogen production with some speculations as to how this has changed from the Archean to present.

The driving force for the deep biosphere

Energy is dissipated from the Earth's core and mantle by the decay of radioactive atoms and crystallization of the outer liquid core. Recent estimates by Hoffmeister & Criss (2005) suggest that the Earth's global heat engine, mainly powered by radioactive decay of uranium and thorium, is 30–32 TW. Potassium in the core is also a significant heat source with an estimated content of the core of 60 to 130 ppm giving off 0.4–0.8 TW of heat (Rama Murthy *et al*. 2003). The heat produced in the Earth gives rise to large-scale dissipative structures in the mantle, which effectively transports the heat to the Earth's mantle–lithosphere boundary. Mantle convection, in turn, shapes the Earth's surface through plate tectonics, which is the dynamic drifting of rigid continental and oceanic lithospheric plates on the mantle (e.g. Condie 1997; Bercovici 2003; Ogawa 2007).

Plate tectonics is mainly driven by the pull exerted by subduction of dense oceanic lithosphere, and in part by the gravitational push of the elevated portion of the plates at ridge crests and shear tractions between the lithospheric plates and the convective mantle (Kearey & Vine 1996; Bercovici 2003; Steiner & Conrad 2007; O'Neill *et al*. 2007). Mid-ocean ridges, which are the divergent plate boundaries, extend for approximately 55 000 km across the ocean floor (Dick *et al*. 2003; German *et al*. 2004), and with spreading rates ranging from ultra slow (<20 mm year^{-1}) to fast ($\sim$80–180 mm year^{-1}), approximately 3.4 km^2 of new oceanic crust is formed every year (Rowley 2002). The ocean floor covers more than two-thirds of the Earth's surface and the bulk of energy dissipated as heat from the Earth is transported by conduction and convection through the seafloor or as extrusion of volcanic rocks. Dissipative structures form where high thermal gradients lead to unstable density stratification of groundwater. Water fluxes that are present in the rocks along mid-ocean ridges are most pronounced at the focused medium- to high-temperature hydrothermal systems. At these sites spectacular chimney structures form and the nutrient-rich solutions mixed with ocean water give rise to rich biological communities (e.g. Baross & Deming 1985; Van Dover 2000; Tarasov *et al*. 2005). Budgets of chemical elements in the ocean water and heat flux estimations suggest, however, that focused flows contribute orders of magnitude less to the overall hydrothermal circulation compared with diffuse flow (de Villiers & Nelson 1999 and references therein). Large-scale diffuse hydrothermal circulation thus has to be taken into account when estimating the global potential of the seafloor to support a hydrogen-driven deep biosphere.

The Earth is divided into compartments with strongly contrasting redox potentials. The core is strongly reduced, the mantle is relatively oxidized, and the crust, hydrosphere and atmosphere today are strongly oxidized (e.g. Jones 2004). Dissipative structures at the interface between the hydrosphere and the lithosphere are places where fresh unaltered mantle or mafic to ultramafic magmatic rocks are in contact with water. Here biochemical reactors may form as microbial communities utilize metastable redox gradients as energy sources. The efficiency of these reactors is dependent on the redox contrast between the rocks and the reacting water. When it comes to the upper mantle and mantle-derived magmatic rocks, data suggests that the oxygen fugacity, a measure of the redox potential, has not changed much for 3.5 Ga (Canil 2002; Li & Lee 2004). On the other hand, the redox potential of the atmosphere and hydrosphere have changed dramatically from reduced in the early Archean, to oxidized after the oxidation event at approximately 2.3 Ga ago to present (e.g. Kasting 1993; Catling & Claire 2005; Kump & Barley 2007). There is, however, one feature that ensures a steady supply of metastable redox gradients as long as plate tectonics and condensed water are present, namely the preferential incorporation of ferrous (Fe^{2+}) to ferric (Fe^{3+}) iron into olivine even at high mantle oxygen fugacities. For olivine, the most abundant mineral in the upper mantle, it is energetically favourable to substitute ferrous iron for

https://doi.org/10.1017/S1473550408004205 Published online by Cambridge University Press

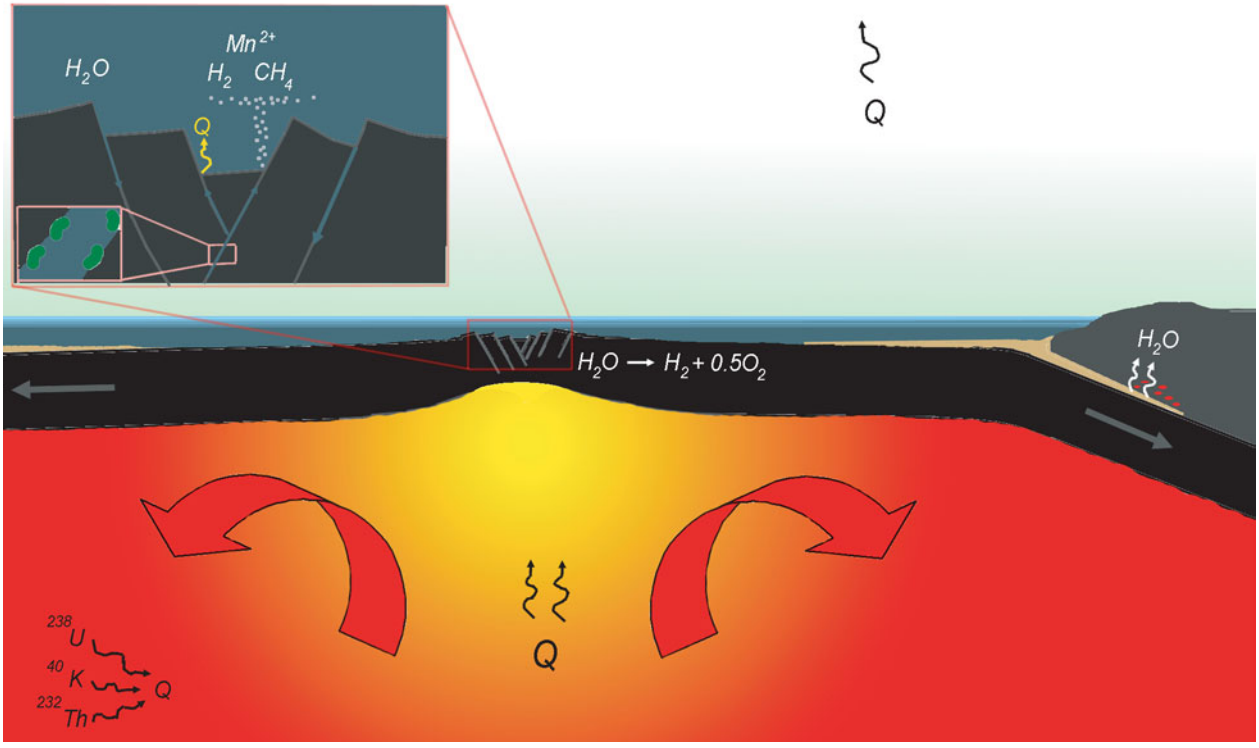


Fig. 1. A summary: Crystallisation of mantle minerals and decay of radioactive elements dominated by thorium and uranium with a significant contribution from potassium produces heat (Q). The heat is dissipated through large-scale convection cells. Plate tectonics driven by subduction of dense lithospheric plates gives rise to divergent and convergent plate boundaries. Heat is dissipated effectively through the former by the formation of hydrothermal convection cells. Ocean water that enters through hydrothermal convection reacts with the crustal and mantle rocks and releases ferrous iron which in turn reduces the water to such an extent that the water decomposes and produces hydrogen ($H_2O \rightarrow H_2 + 0{\cdot}5O_2$). This give rise to a locus of hydrothermal synthesis of organic compounds and metastable redox gradients that supply energy for a dark-powered deep biosphere.

magnesium as they have a similar ionic radius and charge, and only negligible ferric iron is incorporated into the structure (McCammon 2005). As olivine reacts with water, the aqueous solution may be reduced to such a level that hydrogen forms. It does not matter at this point how much oxygen was present initially. Hydrogen forms and oxygen is kept at a level given by the dissociation of water at a given hydrogen activity as long as olivine dissolves in the reduced solution. Dissolution of pyroxenes that contains ferrous iron will contribute to the hydrogen formation, but to a much less extent than olivine. A summary of the driving force powering a deep biosphere residing in the seafloor is illustrated in Fig. 1.

Evidence of H_2 production

The reactions responsible for hydrogen production in the Earth's crust are now well understood based on observations from drill cores, ophiolite outcrops, fluids venting at active hydrothermal sites, laboratory experiments and numerical simulations. This section presents some indirect and direct evidence of hydrogen production in the seafloor and in continental geothermal systems.

Information regarding mineral alteration of the ocean floor is readily available from the ocean drilling program (ODP) reports (e.g. Früh-Green *et al.* 1996a,b; Alt *et al.* 1996a,b; Karson *et al.* 1997; Laverne *et al.* 2001; Alt & Shanks 2003; Bach & Edwards 2003; Bach *et al.* 2006). In order to better understand how seawater interacts with peridotite, drill holes 920B and D were drilled as a part of the ODP Leg 153 at the southern part of the MARK (Mid-Atlantic Ridge, Kane Fracture Zone) area. The two drill holes penetrated 120 and 200 m respectively into the $<$1-Ma-old peridotite with 95% of the recovered rock being serpentinized peridotite. The remaining 5% was variably metamorphosed and altered gabbroic rocks and diabase units (Karson *et al.* 1997). Olivine and pyroxene is altered to serpentine (chrysotile and lizardite) and brucite, with several generations of veins containing serpentine and magnetite plus a later more oxic mineral assemblage which crosscuts the altered peridotite (Dilek *et al.* 1997). The crosscutting relationships indicate a progressive change towards more oxic alteration with time, a feature which is also found in other altered peridotite systems (e.g. DSDP/ODP Leg 209, Site 1268). Important indicators for hydrogen production are local blebs of minerals such as awaruite ($FeNi_3$) and heazlewoodite (Ni_3S_2) that are stable only under very reduced conditions (Alt & Shanks 2003). Hydrogen production is also suggested by carbonate veins enriched in ^{13}C which indicate the formation of methane in the system (Alt & Shanks 2003). Moreover, local differences

https://doi.org/10.1017/S1473550408004205 Published online by Cambridge University Press

in equilibrium-mineral assemblages suggest that the peridotites experienced heterogeneous serpentinization with local variations in fluid fluxes (Alt & Shanks 2003). Textural and compositional relations in altered peridotites from ODP Leg 209, Site 1274, shows how iron substitutes into serpentine minerals and brucite and how this affects the timing of magnetite precipitation (Bach *et al*. 2006). Bach & Edwards (2003) compiled data on the oxidation state of the upper basaltic oceanic crust from a range of DSDP/ODP drill core samples at different ages. Their study suggests that Fe^{3+}/Fe_{tot} increases from 0.15 ± 0.05 to 0.45 ± 0.15 within the first 10–20 Ma. Several lines of evidence indicate that most of the oxidative alteration takes place in young (<10 Ma old) oceanic crust (Bach & Edwards 2003 and references therein).

The most compelling evidence for hydrogen production is available from active hydrothermal vent sites. Two types of peridotite-hosted hydrothermal fields have been recognized based on their temperatures and fluid characteristics (Mével 2003), the high-temperature (360 °C) black-smoker Rainbow type of field, and the low-temperature (40–75 °C) 'white-smoker' Lost City type. These two end-member hydrothermal systems will be reviewed here to illustrate hydrothermal venting characteristics.

The black-smoker type of vent fields was first discovered in 1977 while surveying the Galapagos Rift by the submersible Alvin (Lonsdale 1977; Corliss *et al*. 1979). Since then, many examples of black-smoker systems have been located along the mid-ocean ridges and in back-arc basins (e.g. Binns & Scott 1993; Sudarikov & Roumiantsev 2000; German & Von Damm 2003). The Rainbow hydrothermal field, situated at 36°14′N south of the Amar segment of the Mid-Atlantic Ridge, is hosted in ultramafic rocks and driven by a magmatic heat source (Charlou *et al*. 2002). High-temperature acidic (pH 2.8) fluids with hydrogen concentrations as high as 16 mM emit from vents in this area (Charlou *et al*. 2002). Hydrogen concentrations as well as methane and carbon monoxide are extraordinary high compared with other vent sites along the Mid-Atlantic Ridge. The high hydrogen concentrations are attributed to high-temperature alteration of olivine and orthopyroxene. Abundant linear hydrocarbons up to C_{29} found in the Rainbow system may suggest abiotic Fischer–Tropsch type (FTT) synthesis of organic compounds in this system (Holm & Charlou 2001).

A hydrothermal system radically different from the earlier known black-smoker types of system was discovered in 2000. The new system called the Lost City hydrothermal field is an ultramafic-hosted, low-temperature, high-pH (9.0–9.8) field that builds towering carbonate chimneys (Kelley *et al*. 2001, 2005). Lost City is an off-axis hydrothermal vent field located on 1.5-Ma-old crust, nearly 15 km away from the spreading axis of the Mid-Atlantic Rift (Kelley *et al*. 2001, 2005). Owing to the exothermic nature of serpentinization it has been suggested that hydrothermal systems such as Lost City can be driven partly by the heat released by serpentinization (e.g. Kelley *et al*. 2001; Lowell & Rona 2002; Früh-Green *et al*. 2003). This has important consequences as ultramafic rocks exposed to seawater are common along slow- to ultraslow-spreading mid-ocean ridges (Dick *et al*. 2003). One might thus expect an abundance of ultramafic-hosted hydrothermal systems along such ridges, and this is supported by several recent discoveries of hydrothermal activity at the ultraslow-spreading Arctic Ridges north of Iceland (e.g. Edmonds *et al*. 2003; Pedersen *et al*. 2005, 2007, 2008; Connelly *et al*. 2007).

As for the Rainbow field, fluids emitting from the Lost City show strong evidence of abiotic hydrogen production (Proskurowski *et al*. 2006, 2008). End-member concentrations of vent fluids have hydrogen concentrations from 0.5 to 14.4 mM and methane up to approximately 2 mM (Proskurowski *et al*. 2006). Moreover, low-molecular weight hydrocarbons (C_1 to C_4) venting from the Lost City are suggested to be synthesized by a FTT of reaction (Proskurowski *et al*. 2008).

Several researchers have also argued that continental hydrothermal systems such as in the Yellowstone National Park and in the Columbia River Basalt (CRB) produce hydrogen from strongly reduced geothermal solutions (e.g. Stevens & McKinley 1995, 2000; Spear *et al*. 2005). For instance, hydrogen at concentrations above 300 nM, which is well above the nanomolar concentrations required for energy metabolism (Kral *et al*. 1998), has been recorded in hot springs belonging to the Yellowstone geothermal system (Spear *et al*. 2005). Moreover, the phylogenetic composition of hot-spring communities suggests hydrogen to be the main energy source (Spear *et al*. 2005). Similar micromolar and higher concentrations of hydrogen has been measured from the CRB, which has been attributed to be inorganic formation from water–basalt interactions (Stevens & McKinley 1995, 2000). Experiments on representative basaltic material by the same authors showed that hydrogen forms in appreciable amounts at the alkaline conditions encountered in the CRB for temperatures above 30 °C (Stevens & McKinley 2000). The potential to produce hydrogen from basalt has, however, been contested by Anderson *et al*. (1998, 2001) and the controversy regarding the capability of basalt to support hydrogen-consuming microbial communities will likely go on.

The exact reaction paths for the various systems mentioned above is challenging because of the complex temporal changes and spatial heterogeneities, and one commonly has to rely on indirect measurements (e.g. measurements of vent fluids) and extrapolations. One way to overcome this is to bring the system into the laboratory and run simplified experiments at some well-defined physical conditions (T, P, x). A combination of laboratory experiments and numerical simulations reported by Seyfried *et al*. (2007) has shed more light on both the rates of reactions and the complex nature of serpentinization. Of most interest here is that at the end of a one-year experiment on peridotite alteration at 200 °C and 500 bar they measured hydrogen concentrations in excess of 75 mM. Their numerical simulations however overestimated the hydrogen production with a final concentration of approximately 350 mM. The authors suggest

https://doi.org/10.1017/S1473550408004205 Published online by Cambridge University Press

that this discrepancy is partly due to the incorporation of ferrous iron in the secondary phases and less-efficient conversion of peridotite in the experiment relative to the numerical simulation.

Hydrogen production: how much and how fast?

Hydrogen is observed at up to millimolar concentrations in fluids from focused hydrothermal venting sites at mid-ocean ridges (e.g. Charlou *et al.* 2002; Proskurowski *et al.* 2006). Hydrogen forms at these settings by serpentinization reactions where mafic to ultramafic minerals dissolve and are replaced by a hydrated mineral assemblage consisting of serpentine minerals, oxides etc. (Moody 1976; Sleep *et al.* 2004; Bach *et al.* 2006; Schulte *et al.* 2006; Oze & Sharma 2007). Hydrogen production is linked to the capacity of the rock to reduce the aqueous solution, which is given by the reactivity of the minerals. This is a function of the reaction rate and affinity with respect to the aqueous solution, and the fraction of reductant in the mineral phases. Iron-rich olivines have both reasonably fast reaction rates and contain ferrous iron in a solid-solution between the two olivine end-members fayalite (iron) and forsterite (magnesium). A mid-ocean ridge olivine typically substitutes approximately 10% magnesium for ferrous iron and is called forsterite 90 (Fo90). A general expression for the dissolution of a forsterite with a fraction x of iron substituted for magnesium is given by

$$\mathrm{Fe}_x\mathrm{Mg}_{2-x}\mathrm{SiO_4} + 4\mathrm{H^+} \rightarrow x\mathrm{Fe^{2+}} + (2-x)\mathrm{Mg^{2+}} + \mathrm{SiO_{2,aq}} + 2\mathrm{H_2O}. \quad (1)$$

The magnesium and silica is incorporated into minerals such as brucite, talc, the serpentine minerals chrysotile, lizardite or antigorite and, at low temperatures, zeolites and clay. The exact mineral assemblage is given by the local temperature and pressure (Moody 1976). The ferrous iron released is oxidized to ferric iron by

$$\mathrm{Fe^{2+}} + 0.25\mathrm{O_{2,aq}} + \mathrm{H^+} \leftrightarrow \mathrm{Fe^{3+}} + 0.5\mathrm{H_2O} \quad (2)$$

and the ferric iron speciates according to the solution pH and commonly precipitate magnetite:

$$2\mathrm{Fe^{3+}} + \mathrm{Fe^{2+}} + 4\mathrm{H_2O} \leftrightarrow \mathrm{Fe_3O_4} + 8\mathrm{H^+}. \quad (3)$$

The precipitation of magnetite by reaction (3) consumes ferric iron and indirectly drives the oxygen consumption by reaction (2). Reactions (2) and (3) assume that magnetite is the only mineral that precipitates iron. However, this is not the case as a significant amount of iron is also incorporated in other phases such as brucite and serpentine minerals (Moody 1976; Bach *et al.* 2006; Seyfried *et al.* 2007). This may lead to a reduced activity of the ferrous iron and less consumption of oxygen by reaction (2). In the remaining part of this section, however, we assume the simplified end-member picture that all iron is incorporated into magnetite.

As iron is oxidized, oxygen eventually reaches such a low concentration that water decomposes and produces hydrogen:

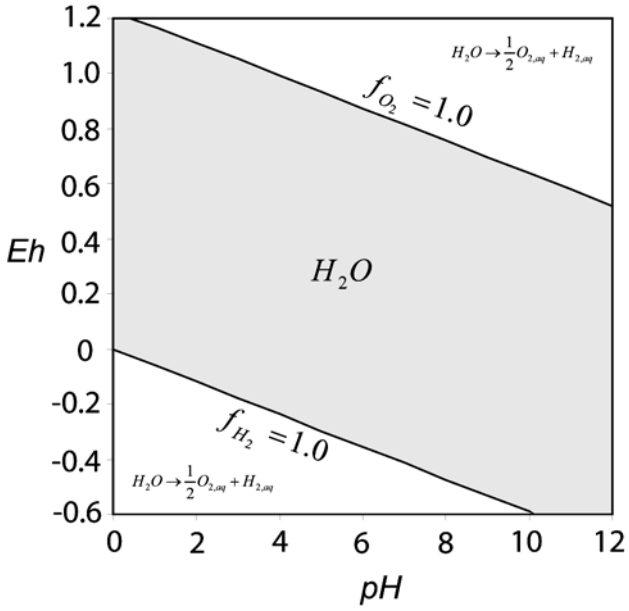


Fig. 2. The stability of water depicted in a pH-pe diagram. Stability limits for water at unit hydrogen fugacity (lower) and unit oxygen fugacity (upper) are shown. Outside these limits water will decompose into molecular hydrogen and oxygen according to $\mathrm{H_2O \rightarrow H_2 + 0{\cdot}5O_2}$.

$$\mathrm{H_2O} \leftrightarrow \mathrm{H_{2,aq}} + 0.5\mathrm{O_{2,aq}}. \quad (4)$$

Fig. 2 shows an Eh-pH diagram that illustrates the stability limit of water. For illustration, two lines bracket the water stability given by unit fugacities of oxygen (upper limit) and hydrogen (lower limit). As the oxygen fugacity decreases according to reaction (2), the equilibrium reaction given by (4) is driven towards the decomposition of water. Thus, hydrogen is produced until the product of hydrogen and oxygen fugacities again satisfy the equilibrium. In Fig. 2 this corresponds to moving the stability of water towards lower Eh at progressively higher hydrogen concentrations. The maximum hydrogen concentration (lowest Eh) possible to achieve at a given temperature, pressure and salinity is given by the bubble point of hydrogen:

$$x_{\mathrm{H_{2,aq}}} = \frac{Py\phi}{K_{\mathrm{H}}\gamma} \cdot \exp\left\{-\frac{\bar{v}}{RT}(P-1)\right\}, \quad (5)$$

where x is mole fraction of hydrogen, P is pressure, y is the fraction of hydrogen in a gas phase, ϕ is the fugacity coefficient, K_{H} is the Henrys law coefficient, γ is the activity coefficient, v is the partial molar volume of hydrogen in water, R is the gas constant and T is temperature.

The local hydrogen concentration is a balance between the reaction rates of the minerals involved and the hydrodynamic conditions. An end-member case is a closed system with no replenishment of the aqueous solution. If also assuming that the product phases are in equilibrium with the water, as is commonly done (e.g. Seyfried *et al.* 2007), then the formation

https://doi.org/10.1017/S1473550408004205 Published online by Cambridge University Press

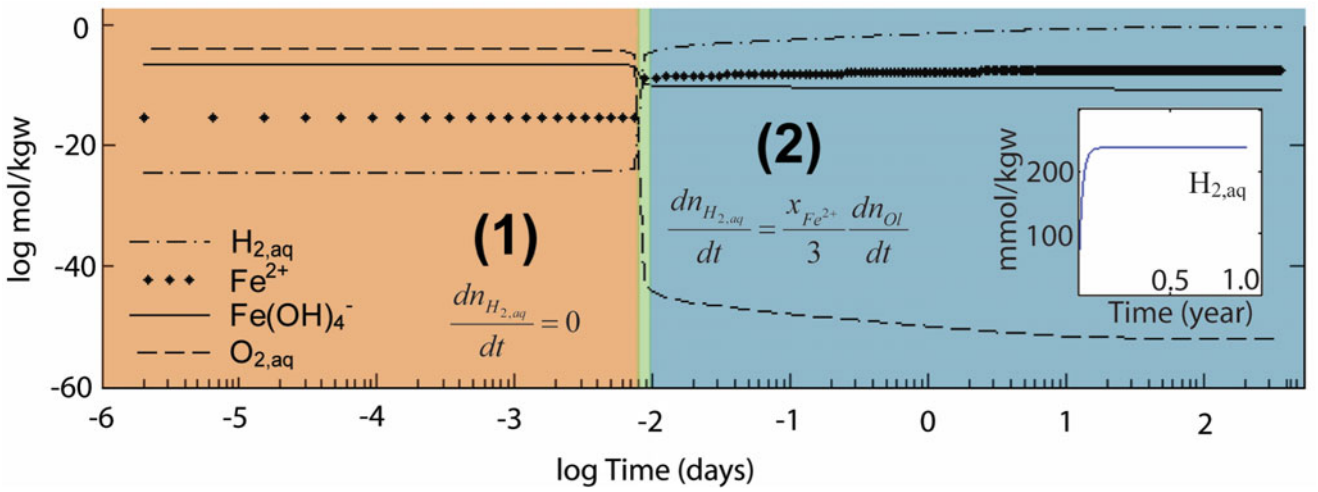


Fig. 3. The temporal reaction progression of 200°C serpentinization of forsterite 91 illustrated by $H_{2,aq}$, $O_{2,aq}$, Fe_{2+} and Fe_{3+} as $Fe(OH)_4$. The progress is divided into two regions: (1) an initial oxidised state where oxidation of ferrous iron consumes oxygen but without exhausting the oxygen, followed by (2) a reduced state that where the oxygen is strongly depleted. The amount of hydrogen that forms, not taking into account ferrous iron incorporation in brucite and serpentine minerals, is for the reduced region equal to $x/3*(dO/dt)$, where x is the fraction of iron in forsterite and dO/dt is the reaction rate.

rate of hydrogen is proportional to the olivine dissolution rate. The rate of olivine dissolution at acidic to basic conditions can be expressed by

$$\frac{dn}{dt} = kS\left(\frac{q}{K} - 1\right) \cdot a_{\mathrm{H}}^{i} \cdot \exp\left(-\frac{Ea}{RT}\right), \tag{6}$$

where k is the far-from-equilibrium dissolution constant (n m^{-2} s^{-1}), S is the reactive surface area (m^2), K is the equilibrium constant for reaction (1), a_H is the proton activity, i is the reaction order with respect to H^+ activity at a given condition, Ea is the apparent activation energy and q is the activity product for reaction (1) given by

$$q = \frac{a_{\mathrm{Fe^{2+}}}^{x} a_{\mathrm{Mg^{2+}}}^{2-x} a_{\mathrm{SiO_{2,aq}}} a_{\mathrm{H_2O}}^{2}}{a_{\mathrm{H^+}}^{4}}. \tag{7}$$

The activity product suggests that with increasing pH, the silica, magnesium and iron concentrations in a closed system will eventually reach saturation with respect to olivine. However, this is not the case because pH will eventually reach a steady-state value given by the steady-state conservation of elements between the reacting olivine and the precipitating phases. The serpentinization is then isochemical except for the uptake of water and release of hydrogen.

To illustrate how olivine dissolution changes the redox state and produces hydrogen, the outcome of a simplified kinetic is shown in Fig. 3. Minerals considered are Fo91, dissolving according to the rate parameters given in (Pokrovsky & Schott 2000) using equation (6), and magnetite, brucite and chrysotile equilibrated with the aqueous solution. Aqueous carbon and iron speciation is taken into account. The system is solved at 200 °C at the vapour pressure of water for 1 year with an initial freshwater solution equilibrated with the equilibrium mineral assemblage. The initial oxygen concentration is 10^{-4} moles kgw^{-1}. Fig. 3 shows how such systems can be divided into two different regions: the first corresponds to an oxidized solution and the second corresponds to the reduced solution. The transition between the two, as oxygen is exhausted, is very rapid. In the first region, olivine dissolution and magnetite precipitation lead to a depletion of oxygen and the amount of hydrogen that forms is not proportional to the amount of ferrous iron supplied by the olivine. This can be expressed by combining reactions (1) to (3) as

$$\mathrm{Fe}_x\mathrm{Mg}_{2-x}\mathrm{SiO_4} + \frac{x}{6}\mathrm{O_{2,aq}} + (4-2x)\mathrm{H^+} \rightarrow \frac{x}{3}\mathrm{Fe_3O_4} + (2-x)\mathrm{Mg^{2+}} + \mathrm{SiO_{2,aq}} + (2-x)\mathrm{H_2O} \tag{8}$$

After the transition, as oxygen is exhausted, decomposition of water has to be taken into account and the combined reactions (1) to (4) now read

$$\mathrm{Fe}_x\mathrm{Mg}_{2-x}\mathrm{SiO_4} + (4-2x)\mathrm{H^+} \rightarrow \frac{x}{3}\mathrm{Fe_3O_4} + (2-x)\mathrm{Mg^{2+}} + \mathrm{SiO_{2,aq}} + \left(2-\frac{4x}{3}\right)\mathrm{H_2O} + \frac{x}{3}\mathrm{H_{2,aq}} \tag{9}$$

At this stage, for each three moles of ferrous iron supplied by olivine, one mole of hydrogen forms. In hydrodynamic settings where local systems are continuously replenished by less-reduced water, a system may stay in the first region and no hydrogen forms as the rock is weathered. This is discussed in more detail below for low-temperature alteration of basalt.

Inorganic synthesis of organic molecules

Hydrothermal formation of hydrogen is important with respect to the biosphere for two reasons: (1) it is a basal part of a present-day deep biosphere (e.g. Stevens 1997; Chapelle *et al.* 2002); and (2) it is an integral component to the hydrothermal synthesis of organic compounds (McCollom *et al.*

https://doi.org/10.1017/S1473550408004205 Published online by Cambridge University Press

1999; Holm & Charlou 2001; Simoneit 2004; McCollom & Seewald 2006) and may thus be a key to the emergence of life on Earth (e.g. Russell 2007; Milner-White & Russell 2008). Thermodynamic calculations by Shock (1990) suggest that the formation of organic molecules in hydrothermal systems is energetically favourable. Experiments at hydrothermal conditions as well as observations of molecules in hydrothermal settings support this.

FTT organic synthesis is a well-known industrial process used to produce hydrocarbons from dry gaseous CO or CO_2 reacted with H_2 over some catalyst (Fischer & Tropsch 1923; Anderson 1984a,b). The outcome of the synthesis is related to the specific catalyst used (Anderson 1984a,b). Abundant organic molecules venting from hydrothermal mounds suggest that FTT synthesis also occurs in the aqueous phase in these settings (e.g. Holm & Charlou 2001; Proskurowski *et al.* 2008). Moreover, experiments at hydrothermal conditions using different catalysts support this (e.g. McCollom *et al.* 1999; Rushdi & Simoneit 2001; Fu *et al.* 2004). For example, aqueous FTT experiments by McCollom *et al.* (1999) and Rushdi & Simoneit (2001) at temperatures between 100 and 400 °C formed a range of different lipid compounds ranging from C_2 to $>C_{35}$, such as n-alkanols, n-alkanolic acids and n-alkenes. By varying the amount of the mineral montmorillonite, McCollom *et al.* (1999) showed that the yield was a function of the amount of mineral catalyst present. Moreover, FTT synthesis in the absence of clay suggested that the stainless steel walls of their reaction vessels also acted as a catalyst. The authors found that the synthesis was most efficient at temperatures between 150 and 250 °C with a maximum yield at around 175 °C (McCollum *et al.* 1999; Rushdi & Simoneit 2001). The formation of lipids in hydrothermal settings has been argued to be of importance for the onset of life in such environments because of their potential for membrane formation (Apel *et al.* 2002; Simoneit *et al.* 2007) and the generation of secondary products such as esters and peptide oligomers (Tsukahara *et al.* 2002). Another series of FTT experiments by Fu *et al.* (2004) used magnetite as a catalyst at 400 °C and 500 bar. From solutions consisting of CO_2 and H_2 they observed reduction of CO_2 to CO and the formation of CH_4 and hydrocarbon compounds.

Hydrogen production through time

The present-day annual hydrogen production can be roughly estimated from: (1) the rate at which new seafloor forms; (2) the average hydration depth; and (3) the fraction of olivine and pyroxene that reacts with time. The potential amount of organic molecules and biomass derived from hydrogen can be estimated in a similar manner.

Based on the area/age versus age distribution of the modern ocean floor, Rowley (2002) estimates a steady seafloor production rate of 3.4 km^2 per year for the last 180 Ma. The maximum depth of alteration can be studied from IODP/DSDP drill cores. A complete section of lavas, dikes and gabbros was drilled during IODP expeditions to Site 1256 in the Eastern Pacific. Cores show abundant iron oxyhydroxizes down to more than 700 mbsf, and pervasive higher-temperature alteration assemblages at depths down to the deepest parts at around 1500 mbsf (Wilson *et al.* 2006). Biotic alteration as traced by alteration textures in glassy pillow lava margins has been found at depths down to more than 500 mbsf (Furnes & Staudigel 1999). The last variable to be taken into account, the weathering rate, can be estimated based on comparisons of oxidized iron Fe^{3+}/Fe^{tot} from seafloor of different ages. Crust that is 118 Ma old sampled at ODP Sites 417/418 shows an average Fe^{3+}/Fe^{tot} of 0.56 (Staudigel *et al.* 1996), whereas 6.6 Ma old crust at ODP Site 504B shows an average value of 0.35 (Bach *et al.* 2003). This suggests that most of the alteration takes place at an early stage with a gradual reduction of alteration rate with age. Based on values such as these, the annual global hydrogen production rate and biomass production from the basaltic seafloor has been estimated by Bach & Edwards (2003). They assumed a seafloor production rate of 3.0 ± 0.5 km^2 per year, a depth of oxidation of 0.5 ± 0.2 km, basalt density of 2950 ± 50 kg m^{-3}, resulting in an upper crust production rate of $4.0 \pm 1.8 \times 10^{12}$ kg per year. From these values an estimated oxidation rate of $1.7 \pm 1.2 \times 10^{12}$ mol Fe per year with 50% of the oxidation attributed to hydrolysis provides $4.5 \pm 3.0 \times 10^{11}$ mol H_2 per year (Bach & Edwards 2003). Thus, the potential chemolithoautotrophic biomass formed from Fe and S oxidation and hydrogen-consuming reactions may be as high as 10^{12} g carbon per year (Bach & Edwards 2003). It has been questioned whether alteration of basalt can lead to high enough hydrogen concentrations to support microbial growth (Anderson *et al.* 1998, 2001). Bach & Edwards (2003) show that if the hydrogen flux is diluted by $4.0 \pm 1.8 \times 10^{15}$ kg seawater per year, which corresponds to a water-to-rock mass ratio of 1000, the average hydrogen concentration will be approximately 100 μM. This should be more than sufficient for a hydrogen-driven community as the lower limit for energy metabolism is of the order of a few nanomolar (Kral *et al.* 1998). However, as Bach & Edwards (2003) also point out, the amount of hydrogen that is introduced into the upper basaltic crust at ridge flanks still remains uncertain. As explained above the progression of olivine (or ocean floor) alteration might be divided into an oxidized or reduced state (Fig. 3). Only in the reduced state will the amount of hydrogen that forms be proportional to the amount of ferrous iron that is released from the rock and oxidize. Given the low content of olivine in basalts relative to ultramafic rocks and the sluggish reaction kinetics of pyroxenes relative to olivine, the latter is nicely illustrated by the experiments by Seyfried *et al.* (2007), it is likely that a large portion of the oceanic seafloor never reaches the strongly reduced state necessary to decompose water to hydrogen. Moreover, the assumption that the ferrous iron is only oxidized by oxygen is likely to fail when nitrate is present in appreciable amounts. Oxidation of ferrous iron by nitrate might prevent the lowest oxygen levels and thus inhibit hydrogen formation.

The majority of the oceanic crust formed today is created at intermediate- to fast-spreading ocean ridges. These ridges

https://doi.org/10.1017/S1473550408004205 Published online by Cambridge University Press

are characterized by a large magma supply which builds a robust thick volcanic pile (Karson 2002). At the other end of the scale is the ultraslow-spreading ridges with a full spreading rate of less than 20 mm per year (Dick *et al*. 2003). At these ridges the magmatic supply is small and tectonic spreading dominates (Dick *et al*. 2003). Amagmatic segments along such ridges have only scattered volcanism and typically expose abundant mantle peridotite (Dick *et al*. 2003). As 20 000 km out of the 55 000 km of the world's oceanic ridges can be characterized as ultraslow-spreading (Dick *et al*. 2003), only a few per cent of the oceanic floor produced annually expose ultramafic rocks. It is, however, likely that the majority of hydrogen production today is focused around the ultraslow-spreading ridges. This might have been different in the Archean seafloor.

Most studies suggest a warmer Archean mantle and a gradual cooling to present (e.g. Abbott *et al*. 1994; Durrheim & Mooney 1994). The consequence of a warmer mantle is that a greater amount of heat dissipated through the crust imposes globally elevated spreading rates or a greater overall ridge length (Karson 2001). Globally elevated spreading rates then leads to even less-exposed mantle rocks relative to volcanics compared with the present day. Melting of a warmer mantle would, however, also imply the formation of more mafic high-magnesium melts (Langmuir *et al*., 1992). Widely acknowledged evidence for this is that high-magnesium ultramafic lavas termed komatiites are only observed in Archean ophiolites such as the type locality in the 3.5 Ga old Barberton Greenstone Belt (Viljoen & Viljoen 1969). Moreover, a more reduced atmosphere and ocean in the Archean as indicated by a wide array of isotopic and mineralogical evidence (e.g. Wiechert 2002; Rouxel *et al*. 2005) mean that, even though less ultramafic rocks were exposed to seawater, even moderate interaction between the reduced seawater and the mafic rocks could potentially produce more hydrogen than on the present seafloor. The Archean ocean would have been close to the reduced state of Fig. 3 and likely produced hydrogen proportionally to the release rate of ferrous iron from the seafloor.

Summary and conclusions

Heat dissipated from the interior of the Earth drives plate tectonics and leads to hydrothermal circulation along plate boundaries and at magmatic active plate interiors. Energy hidden in the chemical potential difference between magmatic minerals and the hydrothermal water is released as the minerals dissolve. Oxidation of released ferrous iron may consume oxygen to such an extent that water decomposes and form molecular hydrogen.

Studies of drill cores, ophiolites, laboratory experiments and numerical simulations suggest that iron-holding olivines are responsible for the bulk of hydrogen production. At present, the largest abundance of olivine is in ultramafic rocks exposed to seawater along the slow- to ultraslow-spreading mid-ocean ridges. The rate of hydrogen formation is controlled by the release rate of ferrous iron from olivine and the fraction of released iron that oxidize. Once hydrogen has reached nanomolar concentrations microbes that reduce components such as carbon dioxide and sulfate can utilize it as a energy source. Moreover hydrogen reacts with carbon through FTT reactions and form organic molecules such as hydrocarbons and lipids. These molecules and others that are formed from hydrogen may have been important as precursor molecules for the onset of life in hydrothermal systems.

Based on numerical simulations on olivine dissolution, the reaction progression is suggested to be divided into two regions based on the oxidation state of the aqueous solution. The first region is characterized by oxygen consumption by the oxidation of ferrous iron without producing hydrogen. After a sharp transition into a reduced solution, the hydrogen production becomes proportional to the amount of ferrous iron released. As basalts have limited reduction capacity, a package of water may reside in the oxidized region throughout its convective travel. The higher reduction capacity of ultramafic rocks leads to a faster progression into the reduced region and significant hydrogen production. A significantly higher global hydrogen production is expected in the Archean because ultramafic lavas such as komatiites may have been abundant. Moreover, a more reduced ocean and atmosphere in the Archean would lead the even higher potential for widespread hydrogen production.

Acknowledgements

I would like to thank Bjarte Hannisdal and Nicola McLoughlin for their helpful comments and reviews. I also acknowledge insightful comments from Gretchen Früh-Green and Ingunn Thorseth. This work was supported by the Research Council of Norway through the BIODEEP project.

References

Abbott, D., Burgess, L., Longhi, J. & Smith, W.H.F. (1994). An empirical thermal history of the Earth's upper mantle. *J. Geophys. Res.* **99**, 13 835–13 850.

Alt, J.C., Teagle, D.A.H., Laverne, C., Vanko, D., Bach, W., Honnorez, J., Becker, K. & Pezard, P.A. (1996a). Ridge flank alteration of upper oceanic crust in the eastern Pacific: a synthesis of results for volcanic rocks of Holes 504B and 896A. *Proc. Ocean Drill. Program: Sci. Results* **148**, 435–450.

Alt, J.C., Laverne, C., Vanko, D., Tartarotti, P., Teagle, D.A.H., Bach, W., Zuleger, E., Erzinger, J., Honnorez, J., Becker, K., Pezard, P.A., Salisbury, M. & Wilkens, R. (1996b). Hydrothermal alteration of a section of upper oceanic crust in the Eastern Equatorial Pacific: a synthesis of results from DSDP/ODP Legs 69, 70, 111, 137, 140, and 148 at Site 504. *Proc. Ocean Drill. Program: Sci. Results* **148**, 417–434.

Alt, J.C. & Shanks, W.C., III (2003). Serpentinization of abyssal peridotites from the MARK area, Mid-Atlantic Ridge: sulfur geochemistry and reaction modeling. *Geochim. Cosmochim. Acta* **67**, 641–653.

Anderson, R.B. (1984a). *The Fischer–Tropsch Synthesis*. Academic Press, New York.

https://doi.org/10.1017/S1473550408004205 Published online by Cambridge University Press

Anderson, R.B. (1984b). Forty years with the Fischer–Tropsch synthesis 1944–1984. *Stud. Surf. Sci. Catalys.* **19**, 457–461.

Anderson, R.T., Chapelle, F.H. & Lovley, D.R. (1998). Evidence against hydrogen-based microbial ecosystems in basalt aquifers. *Science* **281**, 976–977.

Anderson, R.T., Chapelle, F.H. & Lovley, D.R. (2001). Comment on "Abiotic controls on H_2 production from basalt–water reactions and implications for aquifer biogeochemistry". *Env. Sci. Technol.* **35**, 1556–1557.

Apel, C.L., Deamer, D.W. & Mautner, M.N. (2002). Self-assembled vesicles of monocarboxylic acids and alcohols: conditions for stability and for encapsulation of biopolymers. *Biochim. Biophys. Acta* **1559**, 1–9.

Bach, W. & Edwards, K.J. (2003). Iron and sulfide oxidation within basaltic oceanic crust: implications for chemolithoautotrophic microbial biomass production. *Geochim. Cosmochim. Acta* **67**, 3871–3887.

Bach, W., Peucker-Ehrenbrink, B., Hart, S.R. & Blusztjan, J.S. (2003). Geochemistry of hydrothermally altered oceanic crust: DSDP/ODP Hole 504B – implications for seawater – crust exchange budgets and Sr- and Pb-isotopic evolution of the mantle. *Geochem. Geophys. Geosyst.* **4**, DOI: 10.1029/2002GC000419.

Bach, W., Paulick, H., Garrido, C.J., Ildefonse, B., Meurer, W.P. & Humphris, S.E. (2006). Unraveling the sequence of serpentinization reactions: petrography, mineral chemistry, and petrophysics of serpentinites from MAR 15°N (ODP Leg 209, Site 1274). *Geophys. Res. Let.* **33**, L13306, doi:10.1029/2006GL025681, 1–4.

Baross, J.A. & Deming, J.W. (1985). The role of bacteria in the ecology of black-smoker environments. *Biol. Soc. Wash. Bull.* **6**, 355–371.

Bercovici, D. (2003). The generation of plate tectonics from mantle convection. *Earth Planet. Sci. Lett.* **205**, 107–121.

Binns, R.A. & Scott, S.D. (1993). Actively forming polymetallic sulfide deposits associated with felsic volcanic rocks in the eastern Manus back-arc basin, Papua New Guinea. *Econ. Geol.* **88**, 2226–2236.

Canil, D. (2002). Vanadium in peridotites, mantle redox and tectonic environments: Archean to present. *Earth Planet. Sci. Lett.* **195**, 75–90.

Catling, D.C. & Claire, M.W. (2005). How Earth's atmosphere evolved to an oxic state: a status report. *Earth Planet. Sci. Lett.* **237**, 1–20.

Chapelle, F.H., O'Neill, K., Bradley, P.M., Methé, B.A., Ciufo, S.A., Knobel, L.L. & Lovley, D.R. (2002). A hydrogen-based subsurface microbial community dominated by methanogens. *Nature* **415**, 312–315.

Charlou, J.L., Donval, J.P., Fouquet, Y., Jean-Baptiste, P. & Holm, N. (2002). Geochemistry of high H_2 and CH_4 vent fluids issuing from ultramafic rocks at the Rainbow hydrothermal field (36°14′N, MAR). *Chem. Geol.* **191**, 345–359.

Condie, K.C. (1997). Crustal and mantle evolution. In *Plate Tectonics and Crustal Evolution*, Chapter 5. Butterworth-Heinemann, Oxford.

Connelly, D.P., German, C.R., Asada, M., Okino, K., Egorov, A., Naganuma, T., Pimenov, N., Cherkashev, G. & Tamaki, K. (2007). Hydrothermal activity on the ultra-slow spreading southern Knipovich Ridge. *Geochem. Geophys. Geosys.* **8**, Q08013, doi:10.1029/2007GC001652.

Corliss, J.B., Dymond, J., Gordon, L.I., Edmond, J.M., von Herzen, R.P., Ballard, R.D., Green, K., Williams, D., Bainbridge, A., Crane, K. & van Andel T.H. (1979). Submarine thermal sprirngs on the Galápagos Rift. *Science* **203**, 1073–1083.

Cowen, J.P., Giovannoni, S.J., Kenig, F., Johnson, H.P., Butterfield, D., Rappé, M.S., Hutnak, M. & Lam, P. (2003). Fluids from aging ocean crust that support microbial life. *Science* **299**, 120–123.

de Villiers, S. & Nelson, B.K. (1999). Detection of low-temperature hydrothermal fluxes by seawater Mg and Ca anomalies. *Science* **285**, 721–723.

Dick, H.J.B., Lin, J. & Schouten, H. (2003). An ultraslow-spreading class of ocean ridge. *Nature* **426**, 405–412.

Dilek, Y., Coulton, A. & Hurst, S.D. (1997). Serpentinization and hydrothermal veining in peridotites at site 920 in the Mark area. In *Proc. Ocean Drilling Program, Scientific Results*, vol. 153, eds Karson, J.A., Cannat, M., Miller, D.J. & Elthon, D., pp. 35–59.

Durrheim, R.J. & Mooney, W.D. (1994). Evolution of the Precambrian lithosphere: seismological and geochemical constraints. *J. Geophys. Res.* **99**, 15 359–15 374.

Edmonds, H.N., Michael, P.J., Baker, E.T., Connelly, D.P., Snow, J.E., Langmuir, C.H., Dick, H.J.B., Mühe, R., German, C.R. & Graham, D.W. (2003). Discovery of abundant hydrothermal venting on the ultraslow-spreading Gakkel ridge in the Arctic Ocean. *Nature* **421**, 252–256.

Fischer, F. & Tropsch, H. (1923). Preparation of synthetic oil mixtures (synthol) from carbon monoxide and hydrogen. I. *Brennstoff-Chem.* **4**, 276–285.

Fliermans, C.B. (1989). Microbial life in the terrestrial subsurface of southeastern coastal plain sediments. *Hazard. Waste Hazard. Mater.* **6**, 155–175.

Fliermans, C.B. & Balkwill, D.L. (1989). Microbial life in deep terrestrial subsurfaces. *Bioscience* **39**, 370–377.

Früh-Green, G.L., Plas, A. & Dell Angelo, L.N. (1996a). Mineralogic and stable-isotope record of polyphase alteration of upper crustal gabbros of the East Pacific Rise (Hess Deep, Site 894). In *Proc. Ocean Drilling Program, Scientific Results*, vol. 147, eds Mével, C., Gillis, K.M., Allan, J.F. & Meyer, P.S.

Früh-Green, G.L., Plas, A. & Lécuyer, C. (1996b). Petrologic and stable isotope constraints on hydrothermal alteration and serpentinization of the EPR shallow mantle at Hess Deep (Site 895). In *Proc. Ocean Drilling Program, Scientific Results*, vol. 147, eds Mével, C., Gillis, K.M., Allan, J.F. & Meyer, P.S.

Früh-Green, G.L., Kelley, D.S., Bernasconi, S.M., Karson, J.A., Ludwig, K.A., Butterfield, D.A., Boschi, C. & Proskurowski, G. (2003). 30,000 years of hydrothermal activity at the Lost City vent field. *Science* **301**, 495–498.

Fu, Q., Seyfried Jr., W.E. & Horita, J. (2004). Hydrothermal carbon dioxide reduction with magnetite at 400C and 500 bar. In *Proc. 11th Int. Symp. on Water–Rock Interaction*, eds Wanty, R.B. & Seal, R.R.I., pp. 1285–1288. A.A. Balkema, Lisse.

Furnes, H. & Staudigel, H. (1999). Biological mediation in ocean crust alteration: how deep is the deep biosphere? *Earth Planet. Sci. Lett.* **166**, 97–103.

German, C.R. & Von Damm, K.L. (2003). Hydrothermal processes. In *Treatise on Geochemistry*, vol. 6, eds Holland, H.D. & Turekian, K.K., pp. 181–222.

German, C.R., Lin, J. & Parson, L.M. (eds) (2004). *Mid-Ocean Ridges: Hydrothermal Interactions between the Lithosphere and Oceans* (*AGU Geophysical Monograph*, no. 148). American Geophysical Union, Washington, DC.

Hinrichs, K.-U., Hayes, J.M., Sylva, S.P., Brewer, P.G. & DeLong, E.F. (1999). Methane-consuming archaebacteria in marine sediments. *Nature* **398**, 802–805.

Hoffmeister, A.M. & Criss, R.E. (2005). Earth's heat flux revised and linked to chemistry. *Tectonophysics* **395**, 159–177.

Holm, N.G. & Charlou, J.L. (2001). Initial indications of abiotic formation of hydrocarbons in the Rainbow ultramafic hydrothermal system, Mid-Atlantic Ridge. *Earth Planet. Sci. Lett.* **191**, 1–8.

Jiménez, L. (1990). Molecular analysis of deep-subsurface bacteria. *Appl. Environ. Microbiol.* **56**, 2108–2113.

Jones, H.H. (2004). Redox conditions among the terrestrial planets. In *Proc. 35th Lunar and Planetary Science Conf.*, 15–19 March 2004, Houston, TX.

Junge, K., Eicken, H. & Deming, J.W. (2004). Bacterial activity at −2 to −20 °C in Arctic wintertime sea ice. *Appl. Environ. Microbiol.* **70**, 550–557.

Karson, J.A., Cannat, M., Miller, D.J. & Elthon, D. (eds) (1997). *Proc. Ocean Drilling Program, Scientific Results*, vol. 153.

Karson, J.A. (2001). Oceanic crust when Earth was young. *Science* **292**, 1076–1079.

Karson, J.A. (2002). Geologic structure of upper-most oceanic crust from fast- to intermediate-rate mid-ocean ridges. *Annu. Rev. Earth Planet. Sci.* **30**, 347–384.

Kashefi, K. & Lovley, D.R. (2003). Extending the upper temperature limit for life. *Science* **301**, 934.

Kasting, J.F. (1993). Earth's early atmosphere. *Science* **259**, 920–926.

Kearey, P. & Vine, F.J. (1996). *Global Tectonics*, 2nd edn. Blackwell, London.

https://doi.org/10.1017/S1473550408004205 Published online by Cambridge University Press

Kelley, D.S., Karson, J.A., Blackman, D.K., Früh-Green, G.L., Butterfield, D.A., Lilley, M.D., Olson, E.J., Schrenk, M.O., Roe, K.K., Lebon, G.T., Rivizzigno, P. & the AT3-60 Shipboard Party (2001). An off-axis hydrothermal vent field near the Mid-Atlantic Ridge at 30° N. *Nature* **412**, 145–149.

Kelley, D.S. *et al*. (2005). A serpentinite-hosted ecosystem: the Lost City hydrothermal field. *Science* **307**, 1428–1434.

Kimura, H., Asada, R., Masta, A. & Naganuma, T. (2003). Distribution of microorganisms in the subsurface of the Manus Basin Hydrothermal Vent Field in Papua New Guinea. *Appl. Environ. Microbiol*. **69**, 644–648.

Kormas, K.A., Smith, D.C., Edgcomb, V. & Teske, A. (2003). Molecular analysis of deep subsurface microbial communities in Nankai Trough sediments (ODP Leg 190, Site 1176). *FEMS Microbiol. Ecol*. **45**, 115–125.

Kotelnikova, S. & Pedersen, K. (1997). Evidence for methanogenic Archaea and homoacetogenic Bacteria in deep granitic rock aquifers. *FEMS Microbiol. Rev*. **20**, 339–349.

Kral, T., Brunk, K.M., Miller, S.L. & McKay, C.P. (1998). Hydrogen consumption by methanogens on the early Earth. *Origin. Life Evol. Biosph*. **28**, 311–319.

Kump, L.R. & Barley, M.E. (2007). Increased subaerial volcanism and the rise of atmospheric oxygen 2.5 billion years ago. *Nature* **448**, 1033–1036.

Langmuir, C.H., Klein, E.M. & Plank, T. (1992). Petrological systematics of mid-ocean ridge basalts: constraints on melt generation beneath ocean ridges. *Geophys. Monogr*. **71**, 183–280.

Laverne, C., Agrinier, P., Hermitte, D. & Bohn, M. (2001). Chemical fluxes during hydrothermal alteration of a 1200-m long section of dikes in the oceanic crust, DSDP/ODP Hole 504B. *Chem. Geol*. **181**, 73–98.

Li, Z.-X.A. & Lee, C.-T.A. (2004). The constancy of upper mantle f_{O_2} through time inferred from V/Sc ratios in basalts. *Earth Planet. Sci. Lett*. **228**, 483–493.

Lonsdale, P. (1977). Clustering of suspension-feeding macrobenthos near abyssal hydrothermal vents at oceanic spreading centers. *Deep-Sea Res*. **24**, 857–863.

Lowell, R.P. & Rona, P.A. (2002). Seafloor hydrothermal systems driven by the serpentinization of peridotite. *Geophys. Res. Let*. **29**, 1–5.

Lysnes, K., Torsvik, T., Thorseth, I.H. & Pedersen, R.B. (2004). Microbial populations in ocean floor basalt: results from ODP Leg 187. In *Proceedings of the Ocean Drilling Program, Scientific Results*, vol. 187, eds Pedersen, R.B., Christie, D.M. & Miller, D.J.

Marion, G.M., Fritsen, C.H., Eicken, H. & Payne, M.C. (2003). The search for life on Europa: limiting environmental factors, potential habitats, and Earth analogues. *Astrobiology* **3**, 785–811.

McCammon, C. (2005). The paradox of mantle redox. *Science* **308**, 807–808.

McCollom, T.M., Ritter, G. & Simoneit, B.R.T. (1999). Lipid synthesis under hydrothermal conditions by Fischer–Tropsch-Type reactions. *Orig. Life Evol. Biosph*. **29**, 153–166.

McCollom, T.M. & Seewald, J.S. (2006). Carbon isotope composition of organic compounds produced by abiotic synthesis under hydrothermal conditions. *Earth Planet. Sci. Lett*. **243**, 74–84.

Mével, C. (2003). Serpentinization of abyssal peridotites at mid-ocean ridges. *C. R. Geosci*. **335**, 825–852.

Milner-White, E.J. & Russell, M.J. (2008). Predicting the conformations of peptides and proteins in early evolution. *Biology Direct* **3**, doi:10.1186/1745-6150-3-3.

Moody, J.B. (1976). Serpentinizaion: a review. *Lithos* **9**, 125–138.

Nealson, K.H., Inagaki, F. & Takai, K. (2005). Hydrogen-driven subsurface lithoautotrophic microbial ecosystems (SLIMEs): do they exist and why should we care? *TRENDS Microbiol*. **13**, 405–410.

Ogawa, M. (2007). Mantle convection: a review. *Fluid Dyn. Res*., doi: 10.1016/j.fluiddyn.2007.09.001.

O'Neill, C., Jellinek, A.M. & Lenardic, A. (2007). Conditions for the onset of plate tectonics on terrestrial planets and moons. *Earth Planet. Sci. Lett*. **261**, 20–32.

Oze, C. & Sharma, M. (2007). Serpentinization and the inorganic synthesis of H_2 in planetary surfaces. *Icarus* **186**, 557–561.

Parkes, R.J., Cragg, B.A., Bale, S.J., Getliff, J.M., Goodman, K., Rochelle, P.A., Fry, J.C., Weightman, A.J. & Harvey, S.M. (1994). Deep bacterial biosphere in Pacific Ocean sediments. *Nature* **371**, 410–413.

Pedersen, K. (2001). Diversity and activity of microorganisms in deep igneous rock aquifers of the Fennoscandian Shield. In *Subsurface Microbiology and Biochemistry*, eds Fredrickson, J.K. & Fletcher, M., pp. 97–139. Wiley–Liss, New York.

Pedersen, R.B., Thorseth, I.H., Hellevang, B., Schultz, A., Taylor, P., Knudsen, H.P. & Steinsbu, B.O. (2005). Two vent fields discovered at the ultraslow spreading Arctic Ridge System. In *Proc. AGU Fall Meeting 05*, 5–9 December 2005, San Fransisco, CA.

Pedersen, R.B., Thorseth, I.H., Olson, E., Hellevang, H., Okland, I., Baumberger, T., Lilley, M., Bruvoll, V., Mjelde, R. & Haflidason, H. (2007). Hydrothermal activity and core complex formation at the Arctic Mid-Ocean Ridge: an overview of preliminary results of the H2DEEP expedition to the southern Knipovich Ridge at 73N. In *Proc. AGU Fall Meeting 07*, 10–14 December 2007, San Fransisco, CA.

Pedersen, R.B., Barriga, F., Escartin, J., Früh-Green, G., MacLeod, C., Mjelde, R. & Thorseth, I. (2008). Ultra-slow spreading and hydrogen-based deep biosphere: objectives and preliminary results from the H2DEEP project. In *Proc. EGU General Assembly*, 13–18 April 2008, Vienna, Austria (*Geophys. Res. Abstracts*, no. 10).

Pokrovsky, O.S. & Schott, J. (2000). Kinetics and mechanism of forsterite dissolution at 25 °C and pH from 1 to 12. *Geochim. Cosmochim. Acta*. **64**, 3313–3325.

Proskurowski, G., Lilley, M.D., Kelley, D.S. & Olsen, E. (2006). Low temperature volatile production at the Lost City hydrothermal field, evidence from a hydrogen stable isotope geothermometer. *Chem. Geol*. **229**, 331–343.

Proskurowski, G., Lilley, M.D., Seewald, J.S., Früh-Green, G.L., Olson, E.J., Lupton, J.E., Sylva, S.P. & Kelley, D.S. (2008). Abiogenic hydrocarbon production at Lost City hydrothermal field. *Science* **319**, 604–607.

Rama Murthy, V., van Westrenen, W. & Fei, Y. (2003). Experimental evidence that potassium is a substantial radioactive heat source in planetary cores. *Nature* **423**, 163–165.

Roussel, E.G., Cambon bonavita, M.-A., Querellou, J., Cragg, B.A., Webster, G., Prieur, D. & Parkes, R.J. (2008). Extending the sub-seafloor biosphere. *Science* **320**, 1046.

Rouxel, O.J., Bekker, A. & Edwards, K.J. (2005). Iron isotope constraints on the Archean and Paleoproterozoic ocean redox state. *Science* **307**, 1088–1091.

Rowley, D.B. (2002). Rate of plate creation and destruction: 180 Ma to present. *Geol. Soc. Am. Bull*. **114**, 927–933.

Rushdi, A.I. & Simoneit, B.R.T. (2001). Lipid formation by aqueous Fischer–Tropsch-Type synthesis over a temperature range of 100 to 400 °C. *Origin. Life Evol. Biosph*. **31**, 103–118.

Russell, M.J. (2007). The alkaline solution to the emergence of life: energy, entropy and early evolution. *Acta Biotheor*. **55**, 133–179.

Schippers, A., Neretin, L.N., Kallmeyer, J., Ferdelman, T.G., Cragg, B.A., Parkes, J.R. & Jørgensen, B.B. (2005). Prokaryotic cells of the deep sub-seafloor biosphere identified as living bacteria. *Nature* **433**, 861–864.

Schippers, A. & Neretin, L.N. (2006). Quantification of microbial communities in near-surface and deeply buried marine sediments on the Peru continental margin using real-time PCR. *Environ. Microbiol*. **8**, 1251–1260.

Schleper, C., Pühler, G., Kühlmorgen, B. & Zillig, W. (1995). Life at extremely low pH. *Nature* **375**, 741–742.

Schulte, M., Blake, D., Hoehler, T. & McCollom, T. (2006). Serpentinization and its implications for life on the early Earth and Mars. *Astrobiology* **6**, 364–376.

Seyfried Jr., W.E., Foustoukos, D.I. & Fu, Q. (2007). Redox evolution and mass transfer during serpentinization: an experimental and theoretical study at 200 °C and 500 bar with implications for ultramafic-hosted hydrothermal systems. *Geochim. Cosmochim. Acta* **71**, 3872–3886.

Shock, E.L. (1990). Geochemical constraints on the origin of organic compounds in hydrothermal systems. *Orig. Life Evol. Biosph*. **20**, 331–367.

https://doi.org/10.1017/S1473550408004205 Published online by Cambridge University Press

Simoneit, B.R.T. (2004). Prebiotic organic synthesis under hydrothermal conditions: an overview. *Adv. Space Res.* **33**, 88–94.

Simoneit, B.R.T., Rushdi, A.I. & Deamer, D.W. (2007). Abiotic formation of acylglycerols under simulated hydrothermal conditions and self-assembly properties of such lipid products. *Adv. Space Res.* **40**, 1649–1656.

Sleep, N.H., Meibom, A., Fridriksson, Th., Coleman, R.G. & Bird, D.K. (2004). H_2-rich fluids from serpentinization: Geochemical and biotic implications. *Proc. Natl. Acad. Sci. U.S.A.* **101**, 12 818–12 823.

Spear, J.R., Walker, J.J., McCollom, T.M. & Pace, N.R. (2005). Hydrogen and bioenergetics in the Yellowstone geothermal ecosystem. *Proc. Natl. Acad. Sci. U.S.A.* **102**, 2555–2560.

Staudigel, H., Plank, T., While, B. & Schmincke, H.-U. (1996). Geochemical fluxes during seafloor alteration of the basaltic upper oceanic crust: DSDP Sites 417 and 418. In *Subduction Top to Bottom*, eds Bebout, G.E., Scholl, D.W., Kirby, S.H. & Platt, J.P. (*Geophysics Monographs*, vol. 96), pp. 19–38. American Geophysical Union, Washington, DC.

Steiner, S.A. & Conrad, C.P. (2007). Does active mantle upwelling help drive plate motions? *Phys. Planet. Inter.* **161**, 103–114.

Stevens, T.O. & McKinley, J.P. (1995). Lithoautotrophic microbial ecosystems in deep basalt aquifers. *Science* **270**, 450–454.

Stevens, T. (1997). Lithoautotrophy in the subsurface. *FEMS Microb. Rev.* **20**, 327–337.

Stevens, T.O. & McKinley, J.P. (2000). Abiotic controls on H_2 production from basalt–water reactions and implications for aquifer biogeochemistry. *Environ. Sci. Technol.* **34**, 826–831.

Sudarikov, S.M. & Roumiantsev, A.B. (2000). Structure of hydrothermal plumes at the Logatchev vent field, 14°45′N, Mid-Atlantic Ridge: evidence from geochemical and geophysical data. *J. Volc. Geotherm. Res.* **101**, 245–252.

Tarasov, V.G., Gebruk, A.V., Mironov, A.N. & Moskalev, L.I. (2005). Deep-sea and shallow-water hydrothermal vent communities: two different phenomena? *Chem. Geol.* **224**, 5–39.

Teske, A., Ashita, D. & Sogin, M.L. (2003). Genomic markers of ancient anaerobic microbial pathways: sulfate reduction, methanogenesis, and methane oxidation. *Biol. Bull.* **204**, 186–191.

Toffin, L., Webster, G., Weightman, A.J., Fry, J.C. & Prieur, D. (2004). Molecular monitoring of culturable bacteria from deep-sea sediment of the Nankai Trough, Leg 190 Ocean Drilling Program. *FEMS Microbiol. Ecol.* **48**, 357–367.

Torsvik, V. & Øvreås, L. (2008). Microbial diversity, life strategies, and adaption to life in extreme soils. In *Microbiology of Extreme Soils. Soil Biology*, eds Dion, P. & Nautiyal, C.S., pp. 15–43. Springer, Berlin.

Tsukahara, H., Imai, E.I., Honda, H., Hatori, K. & Matsuno, K. (2002). Prebiotic oligomerization on or inside lipid vesicles in hydrothermal environments. *Orig. Life Evol. Biosph.* **32**, 13–21.

Van Dover, C.L. (2000). *The Ecology of Deep-sea Hydrothermal Vents*. Princeton University Press, Princeton, NJ.

Ventosa, A., Arahal, D.R. & Volcani, B.E. (1999). Studies on the microbiota of the Dead Sea – 50 years later. In *Microbiology and Biogeochemistry of Hypersaline Environments*, ed. Oren, A., pp. 139–147. CRC Press, Boca Raton, FL.

Viljoen, M.J. & Viljoen, R.P. (1969). The geology and geochemistry of the lower ultramafic unit of the Onverwacht Group and a proposed new class of igneous rocks. In *Proc. Upper Mantle Project, South African National Committee Symp.* (*Geological Society South Africa Special Publication*, vol. 2), pp. 55–85.

Wiechert, U.H. (2002). Earth's early atmosphere. *Science* **298**, 2341–2342.

Wilson, D.S. *et al.* (2006). Drilling to gabbro in intact ocean crust. *Science* **312**, 1016–1020.

Wortmann, U.G., Chernyavsky, B., Bernasconi, S.M., Brunner, B., Böttcher, M.E. & Swart, P.K. (2007). Oxygen isotope biogeochemistry of pore water sulfate in the deep biosphere: dominance of isotope exchange reactions with ambient water during microbial sulfate reduction (ODP Site 1130). *Geochim. Cosmochim. Acta.* **71**, 4221–4232.

https://doi.org/10.1017/S1473550408004205 Published online by Cambridge University Press